Energy 231 (2021) 120910

Contents lists available at ScienceDirect

Energy

journal homepage: www.elsevier.com/locate/energy

Analysis of the performance of the multi-objective hybrid hydropower-photovoltaic-wind system to reduce variance and maximum power generation by developed owl search algorithm

Xiaojun Ren [a, c], Yongtang Wu [a, c, *], Dongmin Hao [b], Guoxu Liu [a, c], Nicholas Zafetti [d]

[a] Blockchain Laboratory of Agricultural Vegetables, Weifang University of Science and Technology, Weifang, Shandong, 262700, China
[b] School of Architecture and Art, Weifang University of Science and Technology, Weifang, Shandong, 262700, China
[c] Weifang Key Laboratory of Blockchain on Agricultural Vegetables, Weifang, Shandong, 262700, China
[d] Clemson University, North Charleston, SC, United States

ARTICLE INFO

Article history:
Received 1 November 2020
Received in revised form
10 May 2021
Accepted 11 May 2021
Available online 18 May 2021

Keywords:
Renewable sources
Hydropower
Wind energy
Optimization algorithms
Photovoltaic

ABSTRACT

The use of renewable resources to generate energy is one of the most important policy goals in the energy sector. One method to use renewable resources is to apply integrated systems. In this study, an optimal multi-objective integrated system has been applied to power generation. The proposed system includes wind turbines, hydroelectric power plants, and photovoltaic systems. To achieve maximum power generation with minimum fluctuations, a Developed Owl search algorithm (DOSA) with three pareto front solutions has been used. Also, the efficiency of the integrated system in different climate conditions is evaluated. The results of the pareto front show that the developed owl search algorithm is the closest algorithm to the pareto front. Therefore, it is the most accurate to improve the overall multi-objective integrated system. Among pareto front solutions, the second solution provides acceptable results for increasing power generation and reduction of fluctuations. Also, the results of the evaluation of the efficient integrated system in different climate conditions show that in wet conditions when solar radiation and wind are reduced, hydropower causes current to continue in the system by generating electricity and compensating for wind and PV energy loss.

1. Introduction

Today, one of the proposed solutions to the energy crisis is the use of renewable energy that can improve the primary energy use resources [1]. Renewable energy is obtained from reversible sources that can be renewed in a short time by natural sources such as sunlight, wind, wave rain, tides, and global warming [2,3]. Electricity generation by renewable energy is important due to its positive effects on reducing environmental pollution [4,5]. By developing the needs of countries the use of renewable energy sources in the world has an increasing trend [6,7]. According to politicians' plans, renewable energy will contribute more to the energy supply in the future [8,9].

One of the suitable renewable energy resources is the use of solar energy to supply electricity. One of the systems that can directly convert solar energy into electrical energy is the photovoltaic system [10,11]. Photovoltaic systems have unique advantages such as less environmental and industrial pollution, no need for a grid, and somewhat lower maintenance costs [12,13]. Another renewable energy resource is wind energy. Wind energy can be converted into mechanical energy using horizontal or vertical wind turbines [14,15]. According to available statistics, the production of each kWh of electricity from the wind can prevent the release of about 1 kg of CO_2 compared to fossil fuel power plants [16]. Wind and solar energy, which by their very nature are unpredictable and change rapidly under the influence of climate, which can cause problems in electricity generation [17]. Among renewable energies, hydropower plants are more stable and show fewer changes in the face of climate change [18,19]. One method that can control this instability of wind and solar energy in the face of climate change is the integrated use of these energies [20,21]. One integrated system includes two or more renewable energies, each of which produces energy and if one system reduces energy production, the other

* Corresponding author. Blockchain Laboratory of Agricultural Vegetables, Weifang University of Science and Technology, Weifang, Shandong, 262700, China.
E-mail address: wuyongtang1983@126.com (Y. Wu).

https://doi.org/10.1016/j.energy.2021.120910
0360-5442/

Nomenclature table

E_t	total energy generation
E_a	The energy generation arrays of the PV
r_a	The value of solar radiation on the surface of arrays
r_{sd}	The value of solar radiation under standard experimental conditions
t_p	PV system temperature in C°
t_{sd}	Standard experimental conditions temperature that is about to 25 C°
r_d	The average daily intensity of solar radiation on the horizontal surface of NASA
β	The hourly angle of solar radiation relative to the horizon of NASA
$t_{sunrise}$	Sunrise time
P_{EST}	The estimated power in W
ΔH	The different headwater
P_{hydro}	Hydropower generation
η	Generator efficiency
ρ	Density of water
g	Acceleration of gravity is 9.8 m/s^2
Q	The value of discharge m^3/s
W_n	Initial water storage
W_{n+1}	Water storage
F_i	Inlet flow
P_t	All power production of the integrated system
$\overline{P}$	Mean power generation
t_{sunset}	sunset time
C_e	The energy coefficient of the wind turbine
ρ	Water density
A	The area
v_w^3	The wind speed
P	The power generation
V_{cut-in}	The cut-in velocity m/s
$V_{cut-out}$	The cut-out velocity in m/s
V_{EST}	The estimated speed in m/s
F_o	Outlet flow
Q	Discharge flow
Δt	The time phase of reservoir operation
H_{minmum}	The minimum height of the reservoir
$H_{maximum}$	The maximum height of the reservoir
$F_{O\ (minimum)}$	The minimum outflow of the reservoir
$F_{O\ (maximum)}$	The maximum outflow of the reservoir
$P_{minimum}$	The minimum power production
$P_{maximum}$	The maximum power generation
T_t	All of time is calculated
P_H	Power generation hydroelectric system
P_w	The power generation wind turbine

systems compensate for the reduction of energy [22]. Much research has been done on hybrid systems and their use, including the following.

Velloso et and al [23]. investigated the generation of electricity from a combined system that includes solar and water energy sources in the semi-arid area of Brazil. The results showed that the photovoltaic system saves water use in the hydropower plant. It also reduces greenhouse gas emissions in thermal power plants. According to the results of this hybrid system in the period 2013 to 2015, the photovoltaic system adds about 8350 GWh to the actual power produced. Also, power generation by the hybrid system reduces about 28.10% of the amount of CO_2 emitted by thermal power plants.

Al-Turjman et and al [24]. analyzed the feasibility of a combined PV-wind system for home use. In this research, an integrated system has been created using MATLAB software to show the possible output power for loading. The results present that the integrated system presents alternative reasons for consumers and is economically reasonable.

Wei et and al [25]. tested the short-term optimal performance of the integrated hydropower-wind-photovoltaic system helping modified generative adversarial networks. Results explained that the potential for large-scale use of only a combined hydropower-solar-wind system to supply the demand of power transmission is consistent with the direction of the operation strategy, and the operation of the combined system can be improved by increasing the quality scenarios of the suggested deep neural network.

Sultan et and al [26]. studied the design and assessment of an integrated system that includes a photovoltaic and wind and system hydropower pumped storage. The results showed that the integrated system can reduce energy exchange. It also increases the stored ability of the water pump.

Diab et and al [27]. researched the optimal measurement of a solar-wind-hydropower hybrid system in Egypt using various meta-innovative methods. The objective of the optimization method in this research is to reduce the energy cost of the integrated system to reduce the energy fluctuation generated through the photovoltaic-wind integrated system while increasing the power supply reliability of the hybrid system. The optimization results explained that the WOA algorithm has acceptable results compared to other methods.

In the mentioned researches, optimization has been used to improve the results of the integrated system. the optimization algorithms can increase the efficiency of the optimal multi-objective integrated system. Nevertheless, the optimization algorithm has several shortcomings including stuck in the local optimum and premature convergence. The novelty of this research suggests a new optimization method to refine these shortcomings. This suggested algorithm is a new version of the Developed Owl search algorithm (DOSA) to optimize the multi-objective integrated system. Also, in this research, to evaluate the power generation efficiency of the multi-objective integrated system, it is analyzed in different climate conditions to ensure the continuity of electricity flow in different hydrological conditions.

1.1. Case study

Xinjiang is one of the largest provinces in China. Xinjiang is located in western China. Xinjiang is known for its strong winds and rich sources of solar energy. The climate of this province is very hot in summer and is cold in winter. The annual average for the last 22 years of temperature, solar radiation, wind, and precipitation is 5.05 C°, 4.39 kWh/m^2/day, 3.97 km/s, and 165 mm, respectively. The Jilintai I dam has been located in the Kash river, in Xinjiang province. The dam has been installed to generate hydropower. The capacity of this hydroelectric system is about 460 MW. The coordinate-system this hydropower station is 43° 51′ 40″ N, 82° 50′ 51″ E. Dabancheng is a wind farm in Xinjiang province. The total power generation of this farm is about 640 MW. Fig (1) shows the location of Xinjiang and the Jilintai I dam.

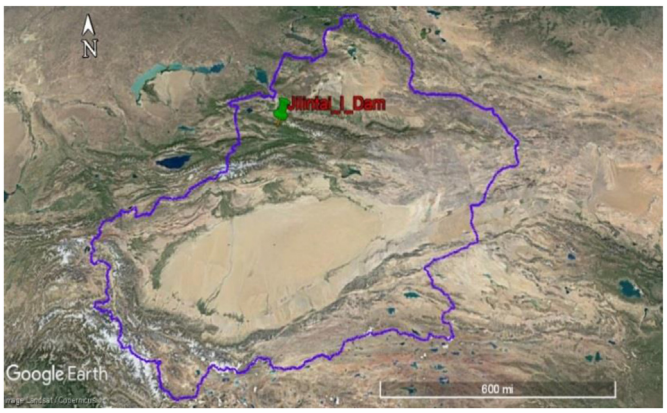

Fig. 1. Location of case study regions.

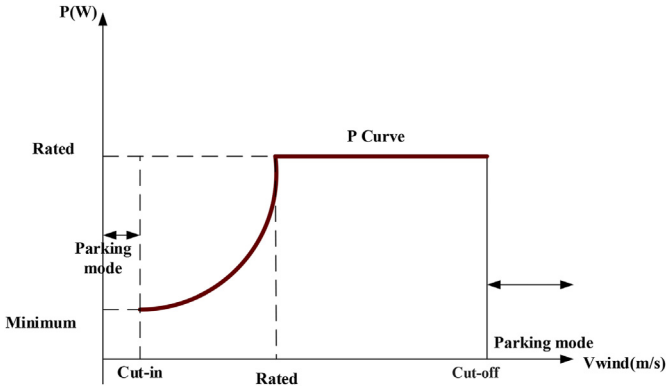

Fig. 2. Wind turbine characteristics curves against wind speed.

2. Method and material

2.1. Calculation of PV system energy generation

PV power voltage changes at various intensities of the solar radiation and temperature [28,29]. If the PV array fails to detect changes in the external environment on time, the total energy PV system efficiency will decrease [30,31]. Therefore, the PowerPoint Maximum Tracking Technology (MPPT) has been used to continuously achieve the most output power by PV system [32]. The PV power output can be calculated using the following equations:

$$P_{pv}(t) = \eta\, P_r S_{ra}(t) \tag{1}$$

where, P_{pv} defines the actual output power, Pr shows the rated power generation is 265Wp; η defines the coefficient of energy convert is 0.9; S_{ra} is the solar radiation.

2.2. Evaluation of wind energy generation

The maximum energy that can be produced through a wind turbine is to some extent to the rotor's swept area. The energy produced through the wind turbine can be determined using the following equations [33,34].

$$E = \frac{1}{2} C_e \rho A v_w^3 \tag{2}$$

where, E defines the energy generation of the wind turbine, C_e describes the energy coefficient of the wind turbine, ρ shows density of air that is 1.225 kg/m^3, A shows the rotor swept area in m^2, v_w^3 defines the wind speed in m/s.

The power generated by a wind turbine depends on the three parameters of wind speed: the cut-in speed, the cut-off speed, and the estimated velocity of the wind turbine. If the wind velocity is less than the cut-off velocity, power generation by the wind turbine is negligible. Therefore, in this case, the wind turbine is in a standing position. Also, the wind turbine must be stopped to be safe when wind speeds exceeding the cut-off speed. Because the wind speed changes in acceptable amounts, the power generation will have a cubic relationship against wind speed as shown in the P-curve. In places where the wind blows, the wind speed is between the cut-off value and the estimated value, the power generation is adjusted to the maximum value by controlling the aerodynamic power, as shown in Fig. (2) [35].

This relationship between wind speed and energy generated can be defined as follows [36]:

$$P = \begin{cases} 0 & V_t < V_{cut-in} \\ Pv & V_{cut-in} \le V_t < V_{EST} \\ P_{EST} & V_{EST} < V_t < V_{cut-out} \end{cases} \tag{3}$$

where, P is the power generation by a wind turbine in Watt, V_{cut-in} is the cut-in velocity in m/s, $V_{cut-out}$ is the cut-out velocity in m/s, V_{EST} is the estimated speed in m/s, P_{EST} is the estimated power in Wat and Pv is the non-linear relationship between power generation and wind velocity.

2.3. Calculation of hydropower generation

Water and energy are closely related. Hydropower is energy generated by the moving force of water [37,38]. In a hybrid system, since hydropower is less affected by climate change, it is used to regulate the energy produced by wind and solar [39,40]. The amount of power generation of hydropower depends on two factors: the volume and average hydraulic jump of the reservoir [41,42]. To calculate hydropower generation can use the following equation:

$$P_{hydro} = \eta \rho g \Delta H Q \tag{4}$$

P_{hydro} shows hydropower generation, η describes generator efficiency (1 %–100%), ρ shows the density of water (1000 kg/m^3), acceleration of gravity is 9.8 m/s^2, Q is *the* value of discharge m^3/s, and ΔH shows the average hydraulic jump which is related to the speed of the inlet flow to the turbine. The hydraulic jump is a phenomenon in which part of the potential energy of water is converted into kinetic energy. This parameter calculated by statistical means and referred to as the “design hydraulic jump [43,44].

2.4. Constraints

Hydropower reservoir is used to control floods, water supply, electricity [45,46]. This hydropower reservoir controls flood, water level, reservoir inlet and outlet, water balance [47,48]. In a multi-objective system, the operating constraints of hydropower include the height of the reservoir water, the outflow of the reservoir, and the hydropower production. Each constraint is described in the following equations.

- Water balance:

$$W_n = W_{n+1} + (F_i - F_o - Q) \times \Delta t \quad (5)$$

where, W_n shows initial water storage, W_{n+1} describes final water storage, F_i inlet flow, F_o outlet flow and Q shows discharge flow, and Δt defines the time phase of reservoir operation.

- *Height of the reservoir water:*

$$H_{minmum} \le H \le H_{maximum} \quad (6)$$

where, $H_{minimum}$ is the minimum height of the reservoir water, $H_{maximum}$ shows the maximum height of the reservoir water It is used to control the flows caused by floods and to protect the dam against severe floods.

- The outflow of the reservoir:

$$F_{O(minimum)} \le F_O \le F_{O(maximum)} \quad (7)$$

where, $F_{O\ (minimum)}$ defines the minimum outflow of the reservoir and $F_{O\ (maximum)}$, describes the maximum value outflow of the reservoir.

- power generation:

$$P_{minimum} \le P \le P_{maximum} \quad (8)$$

where, $P_{minimum}$ shows the minimum power production that depends on the type and the feature of the turbine, and $P_{maximum}$ defines the maximum power generation that is adjusted to the potential of the turbine.

2.5. Objective functions

The purpose of designing a hybrid wind-hydropower-photovoltaic system is to reduce the power changes due to climate changes and increase the most power generation of the hybrid system in different weather conditions [49,50].

To ensure smoothness power generation of the combined system, power changes must be minimized. The following equation is used to reduce changes in the power generation of the combined system, which is one of the optimization goals.

$$M_1 = Min \sum_{t=1}^{T} \frac{\left(P_t - \overline{P}\right)^2}{T_t} \quad (9)$$

$$\overline{P_t} = P_{pv} + P_{hydro} + P_w \quad (10)$$

where, T_t define the all of time is calculated, P_t describes the all power production of the integrated system, $\overline{P}$ shows mean power generation, P_{pv} defines power generation PV system, and P_H defines power generation hydroelectric system, and P_w shows the power generation wind turbine.

- The maximum power generation

To increase the all power output of the combined system, the following equation can be used.

$$M_2 = MaxP_t\left(\vec{Q}\right) = Max \sum_{n=1}^{t} \times \Delta t = Max \sum_{n=1}^{t} \left(P_{pv}^t P_{hydro}^t P_w^t\left(\vec{Q}\right)\right) \times \Delta t \quad (11)$$

where, P_t define the whole power generation.

Based on (7) and (8), the discharge reservoir is the variable that can be constrained to optimize the objectives system. It is calculated using the following equation.

$$X = \left(\overline{Q}\right) \quad (12)$$

2.6. Description barn owl and inspiration to optimize

Meta-heuristic algorithms are a sort of technique for solving optimization problems [51,52]. The use of metaheuristics is exponentially increasing to increase the number of NP-hard and complex problems [53,54]. Generally speaking, several metaheuristics have been proposed inspired by biology or social behaviors and competition between creatures and natural phenomena and other behaviors in nature, for solving the optimization algorithms [55]. Intensification and diversification are the most significant features of meta-heuristic techniques [56]. Intensification seeks the most appropriate solutions available and selects the most appropriate candidate positions. Increasing the ability to converge and prevent getting stuck at the local optimal point is an important part of optimization. Numerous algorithms, all inspired by biology, have been proposed for global search. Lately, Jain et al. [57] A new method has been inspired by the biology of the owl search algorithm (OSA) based on the owl hunting method.

2.6.1. Owl search algorithm (OSA)

Like other metaheuristic algorithms, the OSA algorithm acts randomly and starts the algorithm solution by randomly selecting the population. The population in this algorithm displays the situation of owls between the trees the forest as a search space. Given that the number of owls is and dimensional search space is considered d, the random location of owls is given in the n × d matrix as follows:

$$O = \begin{bmatrix} O_{1,1} & \cdots & O_{1,d} \\ \vdots & \ddots & \vdots \\ O_{n,1} & \cdots & O_{n,d} \end{bmatrix} \quad (13)$$

where, matrix element Oi,j defines the jth parameter (dimension) of the ith owl. To make a uniform distributed primary situation has been used in the following equation:

$$O_i = O_l + (O_l + O_u) \times U(0,1) \quad (14)$$

where, $U(0,1)$ shows an evenly distributed random integer that is classified between [0 to 1], and O_u and O_l upward and downward bounds of ith owl O_i in the jth dimension, respectively.

The cost of the position of owls in the forest is determined using a cost function and is obtained as follows in the matrix:

$$f = \begin{bmatrix} f_1([O_{1,1}, O_{1,2}, \cdots, O_{1,d}]) \\ \vdots \\ f_n([O_{n,1}, O_{n,2}, \cdots, O_{n,d}]) \end{bmatrix} \quad (15)$$

The cost of the owl position depends on the intensity of the sounds gained through the ear. In this case, the owl that receives the maximum sound intensity is known as the best owl because the best owl is closer to the target.

The normalized intensity amount data of ith owl is utilized to update the situation and is obtained using the following equation:

$$I_i = \frac{f_i - w}{b - w} \tag{16}$$

where,

$$b = \max_{m \in 1,\ldots,n} f_m \tag{17}$$

$$w = \min_{m \in 1,\ldots,n} f_m \tag{18}$$

Obtain bait distance information for each owl is gained by the following equation:

$$D_i = \sqrt{\sum_i (O_i - L)^2} \tag{19}$$

where, L shows the bait positions which are gained using the fittest owl.

The OSA algorithm assumes that there is one bait (global optimal) in the forest. During the hunt, owls fly slowly towards the prey. The intensity of the change for the ith owl is as follows:

$$C_i = \frac{I_i}{D_i^2} + R_n \tag{20}$$

where, D_i^2 is utilizes instead of $4\pi D_i^2$, and R_n is random sound to present the model more pragmatic.

As bait changes its position, owls must move silently toward the bait. In the OSA algorithm, the change of bait position is obtained based on probability, and therefore the owls' new positions relative to the bait positions are obtained with the following position update mechanism:

$$O_i^{t+1} = \begin{cases} O_i^t + \beta \times C_i \times |\alpha L - O_i^t|, & p_{pm} < 0.5 \\ O_i^t - \beta \times C_i \times |\alpha L - O_i^t|, & p_{pm} \geq 0.5 \end{cases} \tag{21}$$

where, p_{pm} shows the probability of prey change their position, α and β show a uniformly distributed random number that is between 0 and 0.5. The linear reduction constant is 1.9 to 0, respectively. B is a great change that explains the phrase search space exploration. By extending these differences by applying an algorithm, it can be decreased to enhance development. The OSA algorithm has only one variable (β) that causes it more reliable than other algorithms.

2.6.2. Developed owl search algorithm (DOSA)

The Owl Search Algorithm **(OSA)** is one of the newest optimization algorithms but sometimes traps in the local optimum. This defect offers solutions with premature convergence. modifications have been made to resolve the defect of the OSA algorithm that is explained in this section. Recently, with the spread of the effect of nonlinear dynamics in modeling, the use of chaos theory has expanded. Optimization is one of the fields that can be influenced by chaos theory. From the standard OSA, the variable β is the only random amount in the OSA algorithm. Utilizing the variable β in each iteration causes premature convergence. To prevent premature convergence of the system, a chaotic method called singer mapping is used [58,59]. This method is obtained from the unknown variable β as a regular equation as follows:

$$\beta_{i+1} = 1.07\left(7.9\beta_i - 23.3\beta_i^2 + 28.7\beta_i^3 - 13.3\beta_i^4\right) \tag{22}$$

Another way to improve premature convergence in the OSA algorithm is to apply the Lévy flight (LF). This method is extensively employed in optimization algorithms to prevent premature convergence [60]. Random walking is a key part of this approach to properly managing the local search. This method is on gained as follows:

$$Le(w) \approx w^{-1-\tau} \tag{23}$$

$$w = \frac{A}{|B|^{1/\tau}} \tag{24}$$

$$\sigma^2 = \left\{\frac{\Gamma(1+\tau)}{\tau\Gamma((1+\tau)/2)} \frac{\sin(\pi\tau/2)}{2^{(1+\tau)/2}}\right\}^{\frac{2}{\tau}} \tag{25}$$

where, τ shows the LV index that is between the range [0, 2] (here, $\tau = 3/2$ [54]), $A \sim N(0, \sigma^2)$ and $B \sim N(0, \sigma^2)$, w is the step size, $\Gamma(.)$ describes Gamma function, A/B ~ N (0, σ 2) defines that the samples generated from a Gaussian distribution in which average is zero and variance is σ^2, respectively.

Based on the described variables, new locations of the owls are reached using the following equations:

$$O_i^{t+1} = \begin{cases} O_i^t + \beta \times C_i \times |\alpha L - O_i^t| \times Le(\delta), & p_{pm} < 0.5 \\ O_i^t - \beta \times C_i \times |\alpha L - O_i^t| \times Le(\delta), & p_{pm} \geq 0.5 \end{cases} \tag{26}$$

Fig. (3) shows the flowchart of the DOSA algorithm.

2.6.3. The verification of the DOSA algorithm

In this section, the efficiency improved OSA algorithm is examined. To verify the improved OSA algorithm, some standard criteria have been utilized that the results related to the comparison of these function tests are presented in the results section. In this research, four multi-objective test function of WFG_1, $DTLZ_2$, ZDT_3, KUR function has been applied [61,62]. These four multi-objective test functions are defined as the following equation.

- WFG_1 function

WFG function test has been suggested by Huban [63]. The WFG

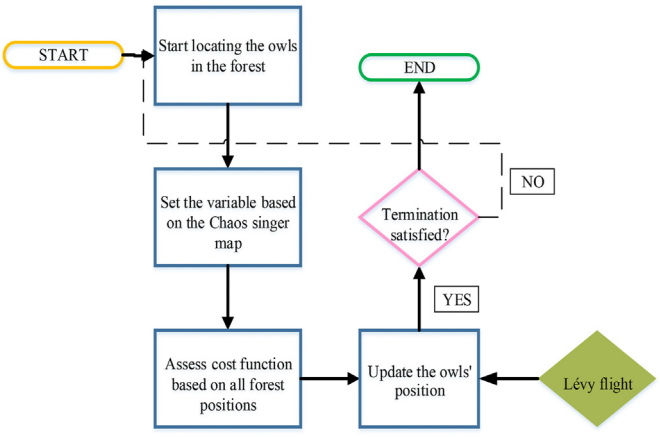

Fig. 3. The flowchart of the developed OSA algorithm.

test function permits a test problem designer to control the characteristics of the test problem by a set of combinable transformations. To make a problem, the test problem designer chooses different shape functions to define the geometry of the fitness space and creates some conversion functions that facilitate the making of transition vectors.

$$\begin{aligned} f_1(x) &= x_M + 2\Pi_{i=1}^{M-1} \sin\left(\frac{X_i\pi}{2}\right) f_{m=2:M-1}(x) \\ &= x_M + 2m\left(\Pi_{i=1}^{M-m} \sin\left(\frac{X_i\pi}{2}\right)\right)\cos\left(x_M - m + \frac{1\pi}{2}\right) f_M(x) \\ &= x_M + 2M\cos\left(\frac{X_1\pi}{2}\right) \end{aligned} \tag{27}$$

- $DTLZ_2$ function

DTLZ test function set, developed by Deb [64]. This test function is not multi-objective, unlike most test problems, because the problems are scalable with any number of objectives. This is an essential feature that has helped numerous studies.

$$\begin{aligned} f_1(x) &= (1+g)\Pi_{i=1}^{M-1} \cos\left(\frac{Y_i\pi}{2}\right) f_{m=2:M-1}(x) \\ &= (1+g)\Pi_{i=1}^{M-m}\cos\left(\frac{Y_i\pi}{2}\right) f_M(x) = (1+g)\sin\left(\frac{Y_1\pi}{2}\right) g \\ &= \sum_{i=1}^{k} (Z_i - 0.5)^2 \end{aligned} \tag{28}$$

- ZDT_3 function

ZDT_3 function has been introduced by Yang [65]. The optimal pareto front of the ZDT_3 function has various interrupted curved sections. Using a sinus function in the ZDT_3 function performs non-continuity on the optimal pareto front, but not in the parameter space. The objective functions of the ZDT_3 are calculated using the following equation.

$$\begin{aligned} f_1\ (x) = x_1\, f_2(x) = g(x)\ \left[1 - \sqrt{\frac{x_1}{g(x)}}\ - \frac{x_1}{g(x)}\ \sin(10\pi x_1)\right]\ g(x) = 1 \\ + 9\left(\sum_{i=2}^{m} x_i\right) \Big/ (m-1) \end{aligned} \tag{29}$$

where, g(x) is determined using the following equation:

- KUR function

KUR test function is offered by Kursawe [66]. The KUR function has two function objectives that are achieved using the following equations.

$$\begin{aligned} f_1(x) = \sum_{i=1}^{m-1}\left(-10\exp\left(-0.2\sqrt{x_i^2 + \sqrt{x_{i+1}^2}}\right)\right) f_2(x) \sum_{i-1}^{m} \\ \left(\left|x_i\right|^{0.8} + 5\sin(x_i)^3\right),\ m = 3 \end{aligned} \tag{30}$$

3. Results and discussion

To optimize the multi-objective hybrid system and to provide maximum total power generation and minimum fluctuations the DOSA algorithm has been used. To analyze the performance of the DOSA algorithm, it is compared with various metaheuristics algorithms. These algorithms are including the Genetic Algorithm (GA) [67], Manta-Ray Foraging Optimization (MRFO) algorithm [68], Shark Smell Optimization (SSO) algorithm [69], Sun Flower Optimization (SFO) algorithm [70], and the basic OSA algorithm. Fig. (4) shows the pareto front of the comparative algorithms.

Based on the suggested method, the best results compared to other algorithms belong to the DOSA algorithm, because it has the best pareto front. Therefore, it has the maximum accuracy compared to the other algorithms. The results show that the DOSA algorithm has the best performance in the process of solving optimization problems. The DOSA algorithm provides the maximum output power for the suggested optimal multi-objective hybrid system compared to other algorithms. Also, the power generation variance by this algorithm is the lowest than other algorithms. Therefore, the electricity generation process is more reliable.

To ensure the efficiency of the suggested multi-objective hybrid system, it has been examined under different climatic conditions. The SPI index is calculated using 22-year data to determine dry and wet periods. To identify different hydrological periods, the SPI index uses precipitation data. The values above zero in the SPI index show precipitation monthly is more than the annual precipitation, and values below zero show precipitation monthly are less than the annual precipitation. According to the SPI index, the dry period occurs when the SPI values below zero (negative value) and the SPI values when is above zero (positive value), that year has been considered as humid period, and if the value of the SPI index is zero or close to zero, that period is called the normal period. Fig. (5) shows the results of the SPI index for the last 22 years.

According to the results of Fig. (5), 2014–2015 has been known as a dry period, 2011–2012 has been known as a wet period. Also, 2018–2019 has been selected as a normal year. In this study, three scenarios have been used. scenario1 shows a wet period, scenario2 shows a normal period, and scenario 3 shows a dry period.

Since the solar radiation, temperature, and wind speed change momentarily. These parameters are calculated daily. Also, since precipitation does not occur on all days of the year, it calculated average monthly. The result of daily solar radiation, temperature, wind speed, and monthly precipitation in different scenarios are shown in Fig. (6-8).

The results showed the intensity of the solar radiation, temperature, wind speed in scenario 3 is most than in scenario 1 and scenario 2. Also, the rainfall value in scenario 1 is most than in scenario 2 and scenario 3. It has been found that the monthly rainfall trend change is not uniform and in some months it has an

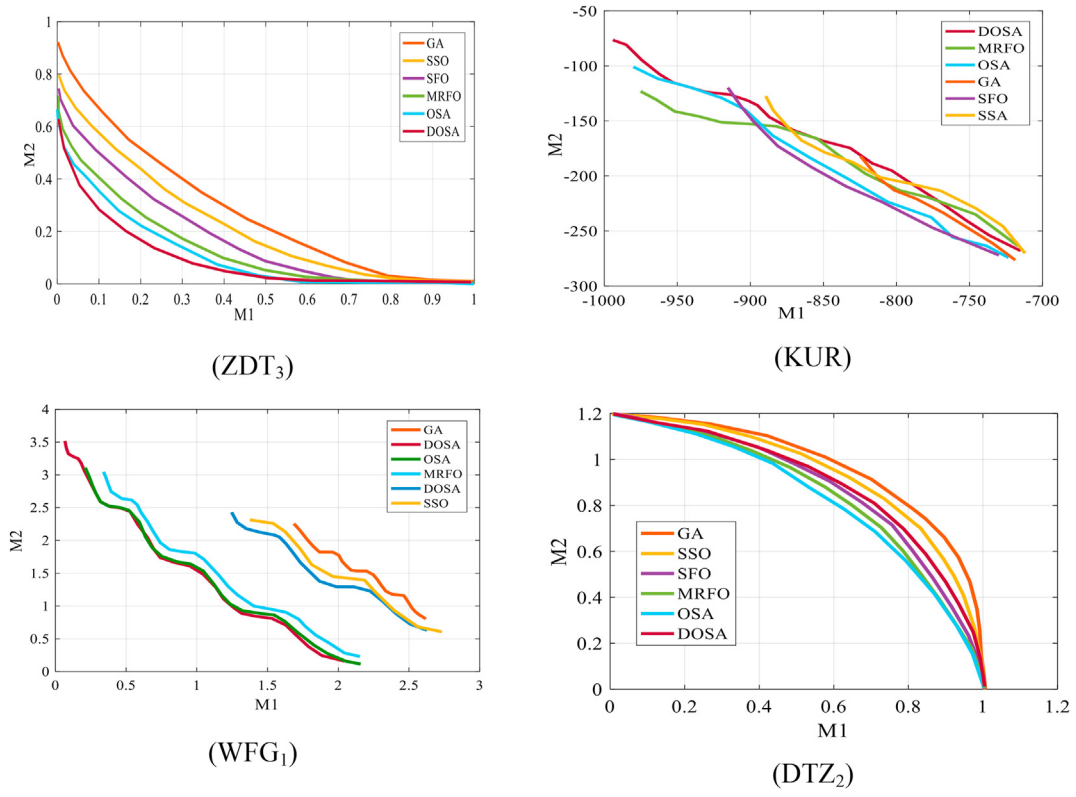

Fig. 4. The results of multi-objective test functions of algorithms.

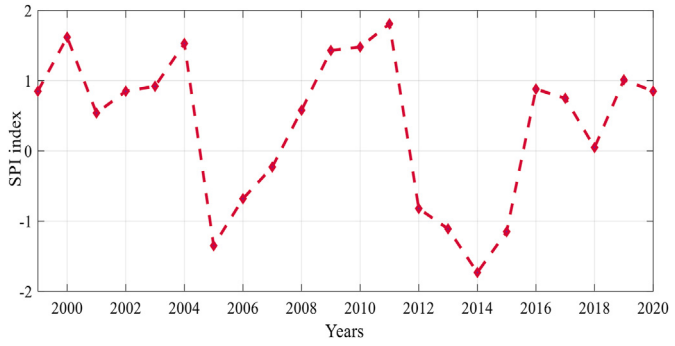

Fig. 5. The SPI index for the last 22 years.

increasing trend and in some months it is a decreasing trend. Seasonal rainfall increases in spring and summer, especially in May, June, and July. Therefore, the probability of seasonal flooding, hence, can lead to an increase in the height of the reservoir hydropower plant. Rainfall in spring and summer has an increasing trend in all scenarios but in scenario1 it is more. Fig. (9) shows the pareto front (A) and three typical solutions (B) for different scenarios.

Fig.9 (A). indicates that the optimal multi-objective hybrid system in scenario1 generates power more than the other scenarios. Also, the power generation variance in scenarios 1 is less than the scenarios 2 and scenarios3. The reason can be the effect of hydropower generation on integrated systems generation. Hydropower generation is more stable compared to photovoltaic and wind turbines. The reason for the stability of hydropower generation is the water reservoir of the hydropower plant, which enables the system to generate electricity in any situation. According to Fig.9 (B). solution1 has minimal power generation, solution2 has middle power generation, and solution3 has maximal power generation, respectively.

Fig. 10–12 shows the result typical solutions and the total power generation by the optimal multi-objective hybrid system in three scenarios.

The results of assessing the integrated system efficiency in different climatic conditions showed that the hybrid system in scenario1 has the maximum power generation and minimum fluctuations compared to other scenarios. In scenario 1, due to the hydropower generation's more impact compared to photovoltaics and wind turbines, the hybrid system generation status is most stable. While in scenario 3, despite the photovoltaics and wind turbines have the most generation than hydropower generation, power fluctuation is the most state. it is due to the instability of wind turbines and photovoltaic generation. However, the hybrid system with the help of photovoltaic and wind turbines and hydropower generation in all climatic conditions and different months of the year can continuously generate electricity. So that in wet conditions, if the photovoltaics and wind turbine generation is

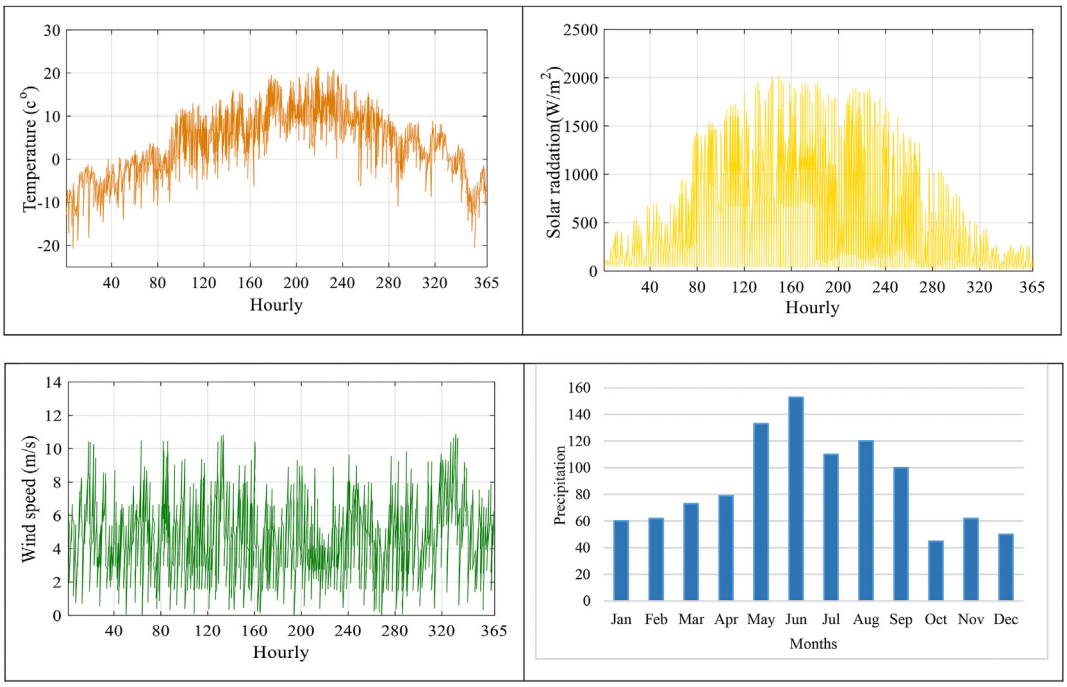

Fig. 6. Climate parameter changes in scenario 1.

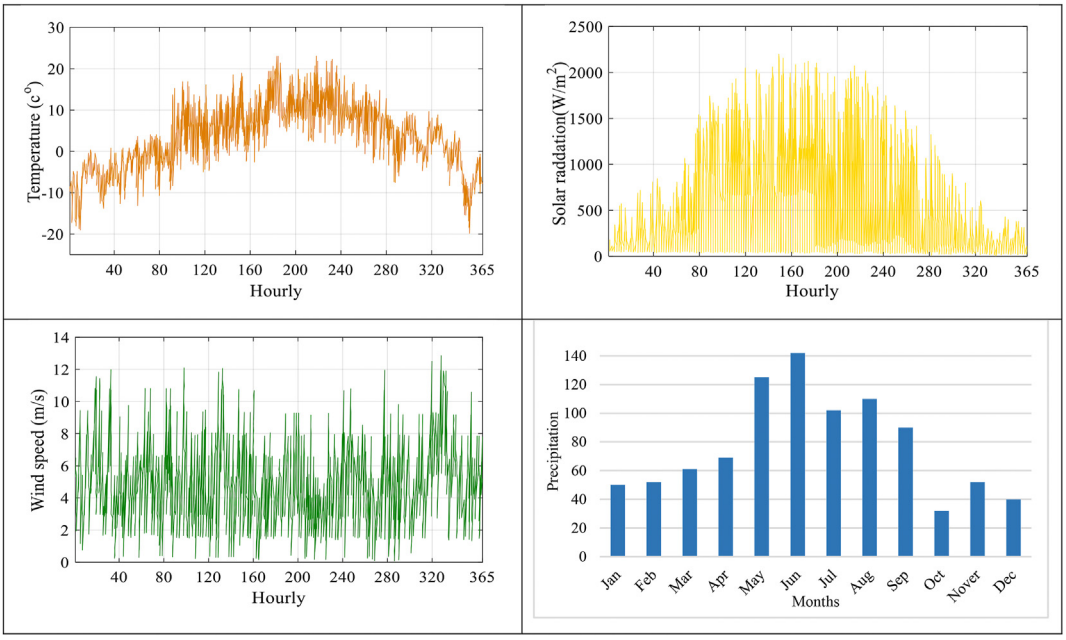

Fig. 7. Climate parameter changes in scenario 2.

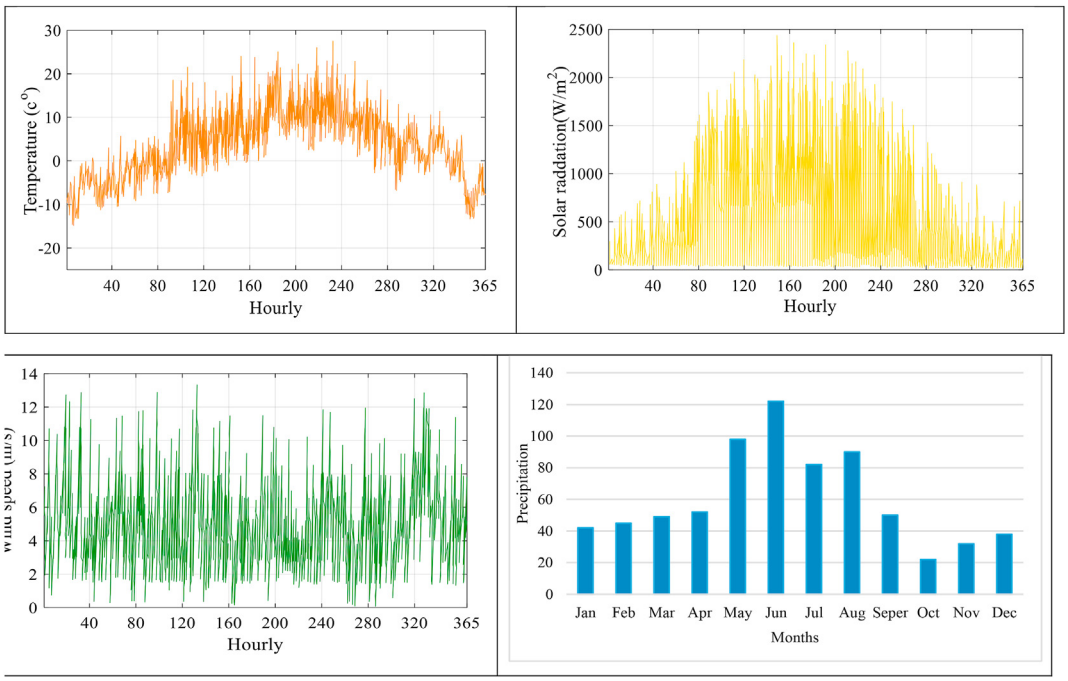

Fig. 8. Climate parameter changes in scenario 3.

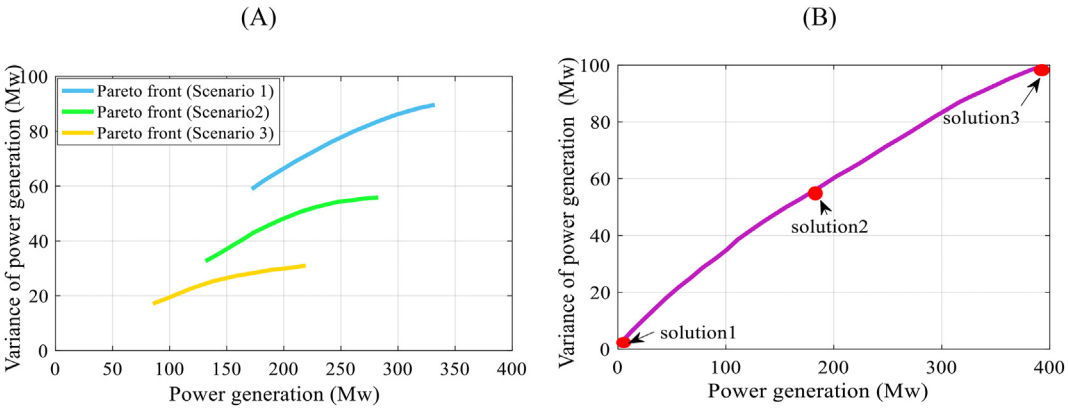

Fig. 9. Optimization results of Pareto Front for different scenarios (A); Pareto Front solutions (B).

reduced, the hydropower system compensates for the lack of power generation. Also, in dry conditions, by reducing the hydropower generation, the photovoltaic system and wind compensate for the reduction of energy. The wind speed and solar radiation in humid conditions are less than in dry periods. Therefore, in the humid year, to compensate for the decrease in production capacity in the photovoltaic system and wind turbines, and to maintain stability and reliability of electricity generation in the electricity network, the electricity generated by the hydropower plant is used.

According to Fig. 10–12, it is clear that as the annual electricity production increases, the output power fluctuations output power increase, which leads to several problems. Therefore, to reduce fluctuations, annual electricity production should be reduced. This reduction in electricity, although it can reduce fluctuations, will not be able to meet the electricity demand. Therefore, in solution 1, it is not able to meet the demand for electricity due to low power generation. Solution 3 is not suitable due to the increase in power fluctuations. Among these solutions, solution 2 has been selected as the most reliable solution among the three solutions. Because it achieves acceptable results from increasing electricity production

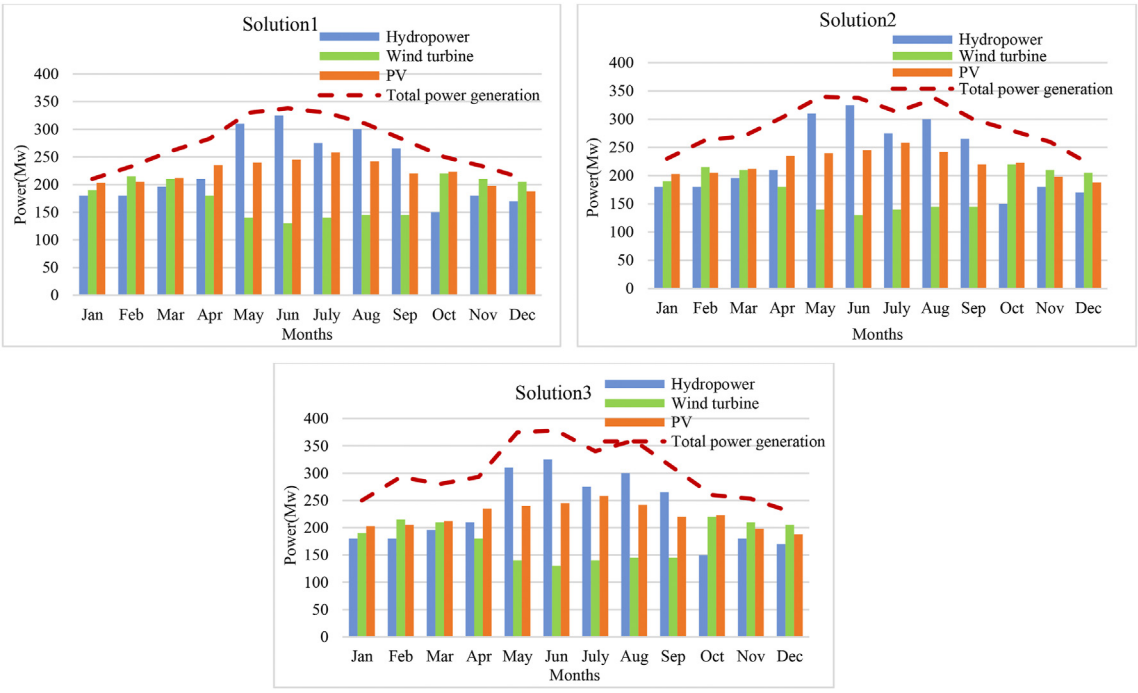

Fig. 10. The total electricity generation of the hybrid system in scenario 1.

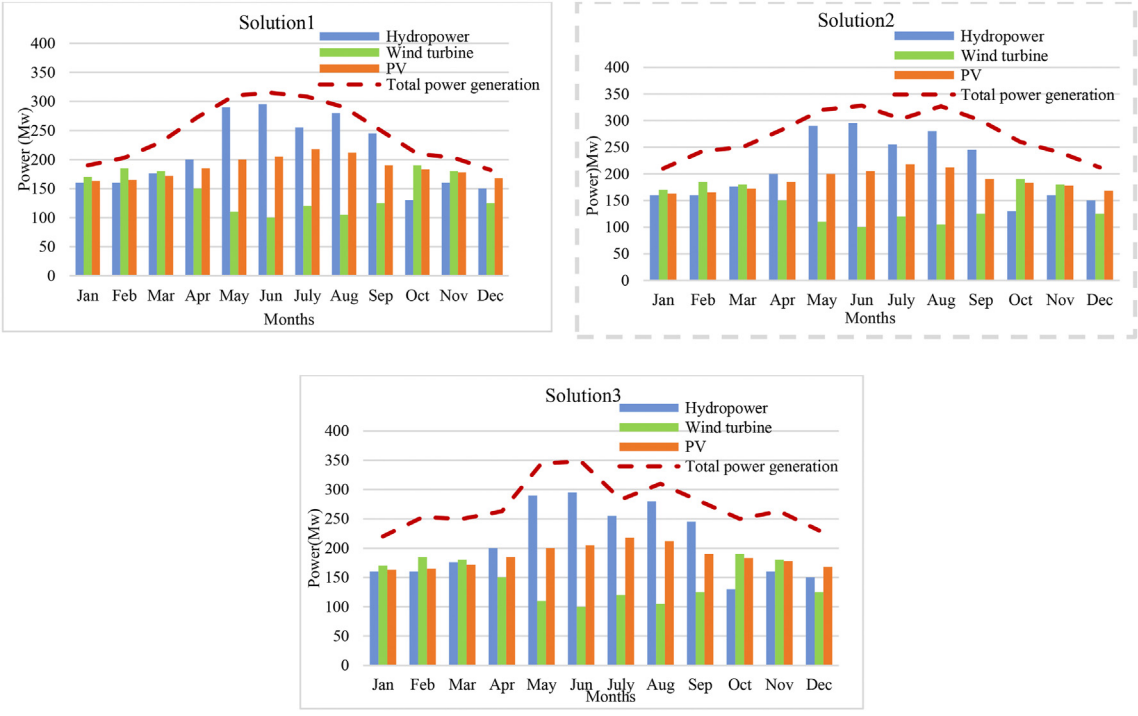

Fig. 11. The total electricity generation of the hybrid system in scenario 2.

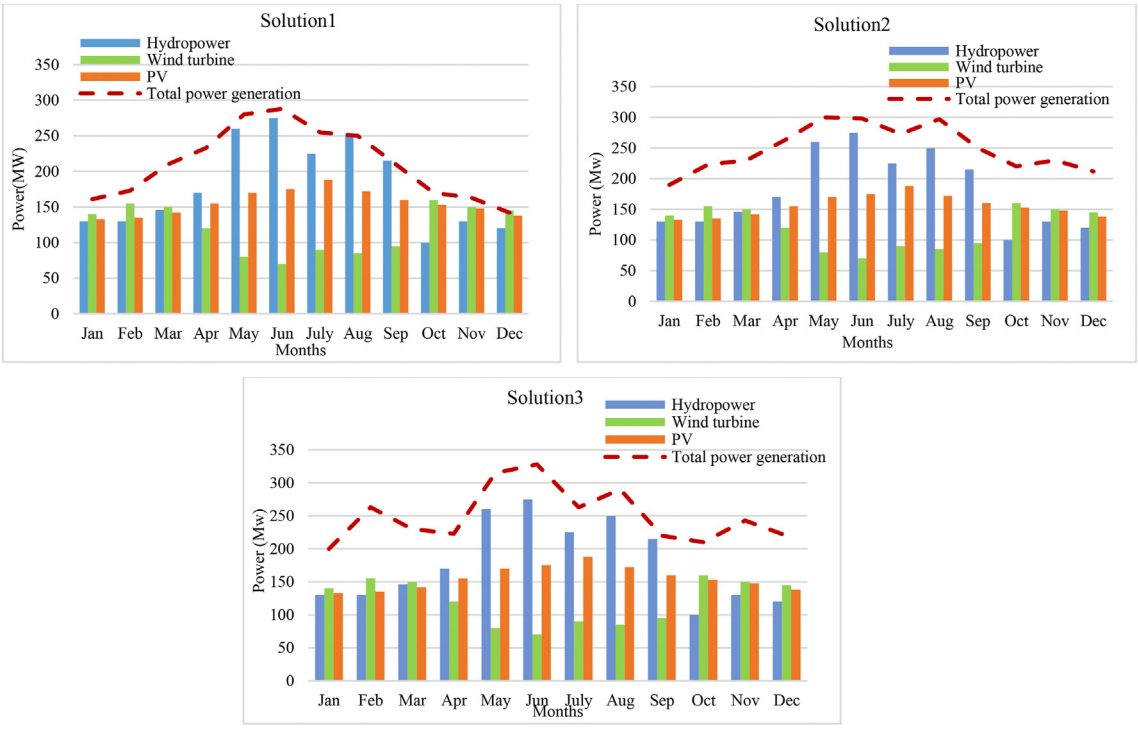

Fig. 12. The total electricity generation of the hybrid system in scenario 3.

and its fluctuations.

4. Conclusion

According to the importance of energy in industry development, this research had been introduced an optimal multi-objective combined system for maximum energy generation. This system was including wind turbines, photovoltaic systems, and hydropower plants. To optimal combined system the new version of the Developed Owl Search Algorithm (DOSA) has been utilized. Also to evaluate the efficiency of the suggested optimal combined system three scenarios have been used. scenario1 showed a wet period, scenario2 showed a normal period, and scenario3 showed a dry period. The results of the performance proposed algorithm showed that DOSA had the best pareto front than other algorithms. The reason is to improve the algorithm and resolve optimization problems such as trapping in optimal local, the imbalance between exploitation and exploration, and premature convergence. Also, the results showed that among the three solutions, solution 2 presented satisfactory results to generate power maximum and fluctuations minimum, because solution 2 has acceptable variances for power generation. Solution 2 can present reasonable and acceptable results for total energy generation. Also, the examination of the efficiency suggested optimal system in different climatic conditions showed that in dry periods, there is a possibility of a shortage for hydropower plant generation, therefore, the photovoltaic system and wind turbines with energy generation compensated for the reduction of total power generation. In the wet period, there is a shortage of energy generation by wind turbines and photovoltaic systems, so hydropower compensated energy loss. Therefore, the use of an integrated system will continue to generate electricity in any climatic conditions. Notwithstanding the favorable performance DOSA algorithm in comparison with other algorithms, since the DOSA algorithm has random nature, it cannot accurately assess the sensitivity. Therefore, to resolve this problem in future work, the DOSA algorithm with classical methods will be used to help give more accurate results.

Author statement

Xiaojun Ren: Conceptualization, Data curation, Writing – original draft, Writing – review & editing. **Yongtang Wu**: Conceptualization, Data curation, Writing – original draft, Writing – review & editing. **Dongmin Hao**: Conceptualization, Data curation, Writing – original draft, Writing – review & editing. Guoxu Liu: Conceptualization, Data curation, Writing – original draft, Writing – review & editing. **Nicholas Zafetti**: Conceptualization, Data curation, Writing – original draft, Writing – review & editing.

Declaration of competing interest

The authors declare that they have no known competing financial interests or personal relationships that could have appeared to influence the work reported in this paper.

References

[1] Alizadeh E, et al. Investigation of contact pressure distribution over the active area of PEM fuel cell stack. Int J Hydrogen Energy 2016;41(4):3062–71.
[2] Akbary P, et al. Extracting appropriate nodal marginal prices for all types of committed reserve. Comput Econ 2019;53(1):1–26.
[3] Knott J, et al. Seasonal and diurnal variation of downstream fish movement at four small-scale hydropower plants. Ecol Freshw Fish 2020;29(1):74–88.
[4] Yuan Z, et al. Probabilistic decomposition-based security constrained transmission expansion planning incorporating distributed series reactor. IET Gener, Transm Distrib 2020;14(17):3478–87.
[5] Muhirwa A, et al. A review on remedial attempts to counteract the power generation compromise from draft tubes of hydropower plants. Renew Energy 2020;150:743–64.
[6] Ye H, et al. High step-up interleaved dc/dc converter with high efficiency. Energy sources, Part A: recovery, utilization, and environmental effects. 2020. p. 1–20.
[7] Liu B, Rodriguez D. Renewable energy systems optimization by a new multi-objective optimization technique: a residential building. J Build Eng 2021;35:

102094.
[8] Jiao P, et al. Multi-objective mean-semi-entropy model for optimal standalone micro-grid planning with uncertain renewable energy resources. Energy 2020;191:116497.
[9] Yu D, Ghadimi N. Reliability constraint stochastic UC by considering the correlation of random variables with Copula theory. IET Renew Power Gener 2019;13(14):2587–93.
[10] Tarafdar HM, Ghadimi N. Radial basis neural network based islanding detection in distributed generation. 2014.
[11] Kececioglu OF, Gani A, Sekkeli M. Design and hardware implementation based on hybrid structure for MPPT of PV system using an interval type-2 TSK fuzzy logic controller. Energies 2020;13(7):1842.
[12] Franzese N, Dincer I, Sorrentino M. A new multigenerational solar-energy based system for electricity, heat and hydrogen production. Appl Therm Eng 2020;171:115085.
[13] Boretti A. Energy storage needs for an Australian National Electricity Market grid without combustion fuels. Energy Storage 2020;2(1):e92.
[14] Liu Y, Wang W, Ghadimi N. Electricity load forecasting by an improved forecast engine for building level consumers. Energy 2017;139:18–30.
[15] Bagal HA, et al. Risk-assessment of photovoltaic-wind-battery-grid based large industrial consumer using information gap decision theory. Sol Energy 2018;169:343–52.
[16] Mehrjerdi H. Modeling, integration, and optimal selection of the turbine technology in the hybrid wind-photovoltaic renewable energy system design. Energy Convers Manag 2020;205:112350.
[17] Yıldız C, et al. A day-ahead wind power scenario generation, reduction, and quality test tool. Sustainability 2017;9(5):864.
[18] Shamel A, Ghadimi N. Hybrid PSOTVAC/BFA technique for tuning of robust PID controller of fuel cell voltage. 2016.
[19] Perera A, et al. Quantifying the impacts of climate change and extreme climate events on energy systems. Nat Energy 2020;5(2):150–9.
[20] Al-Bashir A, et al. Analysis of effects of solar irradiance, cell temperature and wind speed on photovoltaic systems performance. Int J Energy Econ Pol 2020;10(1):353.
[21] Gheydi M, Nouri A, Ghadimi N. Planning in microgrids with conservation of voltage reduction. IEEE Syst J 2016;12(3):2782–90.
[22] Bhayo BA, et al. Power management optimization of hybrid solar photovoltaic-battery integrated with pumped-hydro-storage system for standalone electricity generation. Energy Convers Manag 2020;215:112942.
[23] Velloso MFA, Martins FR, Pereira EB. Case study for hybrid power generation combining hydro-and photovoltaic energy resources in the Brazilian semiarid region. Clean Technologies and Environmental Policy; 2019. p. 1–12.
[24] Al-Turjman F, et al. Feasibility analysis of solar photovoltaic-wind hybrid energy system for household applications. Comput Electr Eng 2020;86:106743.
[25] Wei H, et al. Short-term optimal operation of hydro-wind-solar hybrid system with improved generative adversarial networks. Appl Energy 2019;250:389–403.
[26] Sultan HM, et al. Design and evaluation of PV-wind hybrid system with hydroelectric pumped storage on the National Power System of Egypt. Glob Energy Interconnect 2018;1(3):301–11.
[27] Diab AAZ, Sultan HM, Kuznetsov ON. Optimal sizing of hybrid solar/wind/hydroelectric pumped storage energy system in Egypt based on different meta-heuristic techniques. Environ Sci Pollut Control Ser 2019:1–23.
[28] Jain AA, Rabi BJ, Darly S. Application of QOCGWO-RFA for maximum power point tracking (MPPT) and power flow management of solar PV generation system. Int J Hydrogen Energy 2020;45(7):4122–36.
[29] Jaszczur M, Hassan Q. An optimisation and sizing of photovoltaic system with supercapacitor for improving self-consumption. Appl Energy 2020;279:115776.
[30] Dinulovic D, et al. Dual-rotor electromagnetic based energy harvesting system for smart home applications. IEEE Trans Magn 2020.
[31] Tharo Z, Syahri MA. Combination of solar and wind power to create cheap and eco-friendly energy. IOP conference series: materials science and engineering. IOP Publishing; 2020.
[32] Ge X, et al. Implementation of a novel hybrid BAT-Fuzzy controller based MPPT for grid-connected PV-battery system. Contr Eng Pract 2020;98:104380.
[33] Gumilar L, et al. Analysis curve of maximum power and torque turbine generated by vertical axis wind turbine based on number of blades. AIP conference proceedings. AIP Publishing LLC; 2020.
[34] Leng H, et al. A new wind power prediction method based on ridgelet transforms, hybrid feature selection and closed-loop forecasting. Adv Eng Inf 2018;36:20–30.
[35] Sedaghat A, et al. A new semi-empirical wind turbine capacity factor for maximizing annual electricity and hydrogen production. Int J Hydrogen Energy 11 June 2020;45(32):15888–903.
[36] Chen J, et al. An efficient rotational sampling method of wind fields for wind turbine blade fatigue analysis. Renew Energy 2020;146:2170–87.
[37] Eslami M, et al. A new formulation to reduce the number of variables and constraints to expedite SCUC in bulky power systems. Proc Natl Acad Sci India: Phys Sci 2019;89(2):311–21.
[38] Saeedi M, et al. Robust optimization based optimal chiller loading under cooling demand uncertainty. Appl Therm Eng 2019;148:1081–91.
[39] Hosseini Firouz M, Ghadimi N. Optimal preventive maintenance policy for electric power distribution systems based on the fuzzy AHP methods. Complexity 2016;21(6):70–88.
[40] Gollou AR, Ghadimi N. A new feature selection and hybrid forecast engine for day-ahead price forecasting of electricity markets. J Intell Fuzzy Syst 2017;32(6):4031–45.
[41] Wang Y, Liu J, Han Y. Production capacity prediction of hydropower industries for energy optimization: evidence based on novel extreme learning machine integrating Monte Carlo. J Clean Prod 2020;272:122824.
[42] Zhang Y, et al. Optimization of China's electric power sector targeting water stress and carbon emissions. Appl Energy 2020;271:115221.
[43] Pelz PF, Froehlich T. Free surface influence on low head hydro power generation. IOP conference series: earth and environmental science. IOP Publishing; 2016.
[44] Zhou Y, et al. Uniform flow and energy dissipation of hydraulic-jump-stepped spillways. Water Supply 2020;20(4):1546–53.
[45] Daddi M. Integrating hydrological constraints for hydropower in energy models. The case study of the Zambezi river basin in the Southern African power pool. 2020.
[46] Cai W, et al. Optimal bidding and offering strategies of compressed air energy storage: a hybrid robust-stochastic approach. Renew Energy 2019;143:1–8.
[47] Liu J, et al. An IGDT-based risk-involved optimal bidding strategy for hydrogen storage-based intelligent parking lot of electric vehicles. J Energy Storage 2020;27:101057.
[48] Khodaei H, et al. Fuzzy-based heat and power hub models for cost-emission operation of an industrial consumer using compromise programming. Appl Therm Eng 2018;137:395–405.
[49] Shen J, et al. Multiobjective optimal operations for an interprovincial hydropower system considering peak-shaving demands. Renew Sustain Energy Rev 2020;120:109617.
[50] Meng Q, et al. A single-phase transformer-less grid-tied inverter based on switched capacitor for PV application. J Contr Automat Electric Syst 2020;31(1):257–70.
[51] Yıldız C, Şekkeli M. Optimal bidding in Turkey day ahead electricity market for wind energy and pumped storage hydro power plant. Pamukkale Univ J Eng Sci 2016;22(5):361–6.
[52] Grothe B. How the barn owl computes auditory space. Trends Neurosci 2018;41(3):115–7.
[53] Hamian M, et al. A framework to expedite joint energy-reserve payment cost minimization using a custom-designed method based on mixed integer genetic algorithm. Eng Appl Artif Intell 2018;72:203–12.
[54] Li X, Niu P, Liu J. Combustion optimization of a boiler based on the chaos and Levy flight vortex search algorithm. Appl Math Model 2018;58:3–18.
[55] Cuevas E, Gálvez J, Avalos O. Recent metaheuristics algorithms for parameter identification. Springer; 2020.
[56] Saddique MS, et al. Solution to optimal reactive power dispatch in transmission system using meta-heuristic techniques—Status and technological review. Elec Power Syst Res 2020;178:106031.
[57] Jain M, et al. Owl search algorithm: a novel nature-inspired heuristic paradigm for global optimization. J Intell Fuzzy Syst 2018;34(3):1573–82.
[58] Yang D, Li G, Cheng G. On the efficiency of chaos optimization algorithms for global optimization. Chaos, Solit Fractals 2007;34(4):1366–75.
[59] Rim C, et al. A niching chaos optimization algorithm for multimodal optimization. Soft Comput 2018;22(2):621–33.
[60] Choi C, Lee J-J. Chaotic local search algorithm. Artif Life Robot 1998;2(1):41–7.
[61] Chase N, et al. A benchmark study of multi-objective optimization methods. BMK-3021, Rev 2009;6:1–24.
[62] Bossek J. Smoof: single-and multi-objective optimization test functions. R J 2017;9(1):103.
[63] Huband S, et al. A scalable multi-objective test problem toolkit. International conference on evolutionary multi-criterion optimization. Springer; 2005.
[64] Deb K, Sinha A, Kukkonen S. Multi-objective test problems, linkages, and evolutionary methodologies. Proceedings of the 8th annual conference on Genetic and evolutionary computation. 2006.
[65] Yang X-S, Karamanoglu M, He X. Multi-objective flower algorithm for optimization. Procedia Comput Sci 2013;18:861–8.
[66] Deb K, et al. Scalable multi-objective optimization test problems. In: CEC'02 (cat. No. 02TH8600)Proceedings of the 2002 congress on evolutionary computation. IEEE; 2002.
[67] Holland JH. Genetic algorithms. Sci Am 1992;267(1):66–73.
[68] Zhao W, Zhang Z, Wang L. Manta ray foraging optimization: an effective bio-inspired optimizer for engineering applications. Eng Appl Artif Intell 2020;87:103300.
[69] Abedinia O, Amjady N, Ghadimi N. Solar energy forecasting based on hybrid neural network and improved metaheuristic algorithm. Comput Intell 2018;34(1):241–60.
[70] Qais MH, Hasanien HM, Alghuwainem S. Identification of electrical parameters for three-diode photovoltaic model using analytical and sunflower optimization algorithm. Appl Energy 2019;250:109–17.